Radio galaxies near the epoch of reionisation

Saxena, A.

Author: Saxena, A.
Title: Radio galaxies near the epoch of reionisation
Issue Date: 2019-06-26

1 Introduction

1.1 Historical context

Although several attempts were made to image the sun at radio (meter) wavelengths in the late 19th century, the recent history of radio astronomy begins with the pioneering engineer Karl G. Jansky who began experimenting with detecting radio emission from the sky using an antenna that he built while working for Bell Telephone Laboratories. From his initial observations, Jansky published a series of papers reporting the detection of radio emission from outside the solar system, and specifically from the centre of the Milky Way (Jansky 1933a,b), which failed to attract much attention. Jansky was subsequently reassigned to another project and did no further work in radio astronomy. The field of astronomy would eventually recognise the importance of his work by naming the unit of flux density after him, where 1 Jansky (Jy) = 10^{-26} Watt Hz^{-1} m^{-2}.

Jansky's papers captured the attention of another radio engineer, Grote Reber. In 1937, Reber built what could be attributed as the first ever radio 'telescope', consisting of a 9.5-m parabolic reflector dish, in his backyard and began surveying the radio sky. He corroborated Jansky's detection of radio emission from the Galactic plane and in 1944 Reber published a map of the radio sky finding peaks in emission originating from the constellations of Sagittarius (galactic centre), Cygnus, Cassiopeiae, Canis Major and Puppis (Reber 1944). Only a couple of years later, Hey et al. (1946) reported the detection of radio fluctuations from the constellation Cygnus, which would be the first truly extragalactic source observed at radio wavelengths (Cygnus A).

The end of the Second World War ushered in an era of large-sky radio surveys, primarily led by ex-radar scientists based in Cambridge, Manchester and Sydney. Over the next few decades, these surveys would lead to the discovery of hundreds, and even thousands of radio sources, a large majority of which were extragalactic

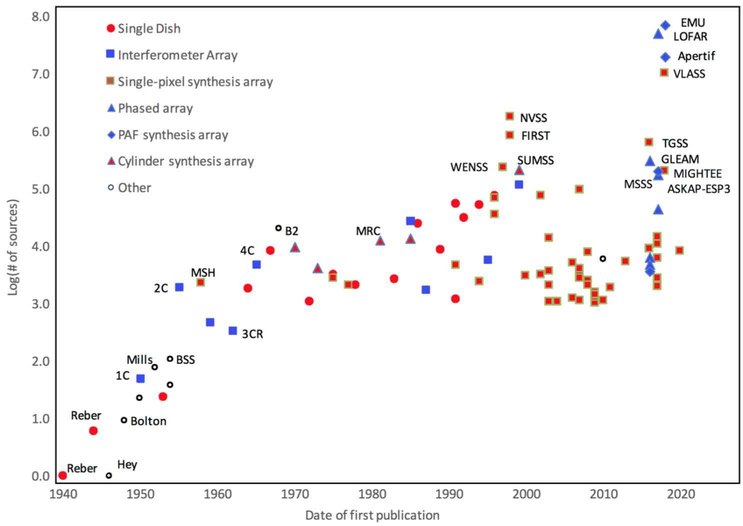

Figure 1.1: Number of known extragalactic radio sources discovered by surveys as a function of time, taken from Norris (2017).

in nature. The best example of one such early survey is the 2C radio survey at Cambridge, that lead to the detection of 1,936 discrete radio sources at an observing frequency of 81 MHz (Shakeshaft et al. 1955). Interestingly, the distribution of radio flux densities of the ‘radio stars’ in this survey was incompatible with the Euclidean distribution of ‘standard candle’ sources in the Universe, and was used to rule out the ‘Steady State’ theory in favour of the ‘Big Bang’ model for the Universe (Ryle & Scheuer 1955). This remarkable result increased radio astronomy efforts all around the world, in the form of the construction of larger telescopes offering higher sensitivities and better angular resolutions. This resulted in a tremendous increase in the number of known radio sources, and the number of radio sources detected in surveys over the last few decades is shown in Figure 1.1 taken from Norris (2017). We draw the attention of the reader that the y-axis of Figure 1.1 is logarithmic.

1.1.1 Radio galaxies

Although radio surveys have led to the discovery of a plethora of radio sources that include radio pulsars, star-forming galaxies, galaxy clusters and the more recently discovered fast radio bursts, the focus of this thesis is on extragalactic active galactic nuclei (AGN) that emit copious amounts of radio emission. The classi-

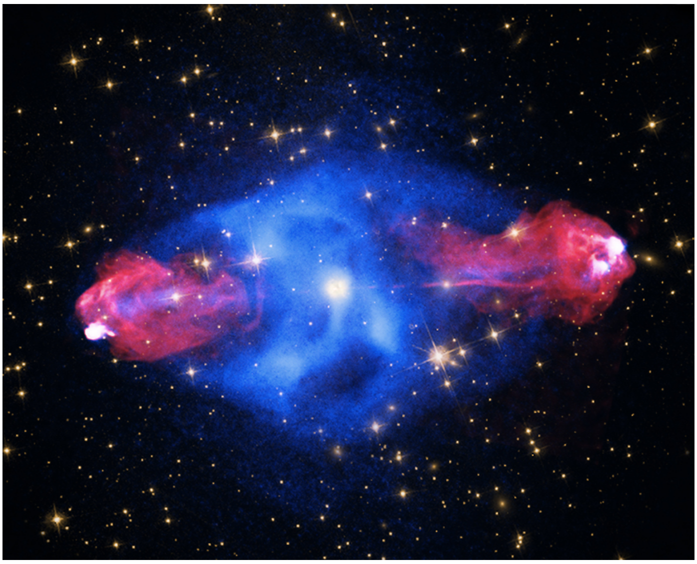

Figure 1.2: Light from Cygnus A at radio (red), X-ray (blue) and optical (background) wavelengths. Cygnus A is a typical twin lobed radio source powered by accretion on to the central SMBH. Image Credit: X-ray: NASA/CXC/SAO; Optical: NASA/STScI; Radio: NSF/NRAO/AUI/VLA. Taken from NASA's Astronomy Picture of the Day, 24 January 2015.

cal 'radio galaxies' discovered in early large-sky surveys usually consisted of two radio 'lobes' that are created by synchrotron radiation from relativistic plasma believed to be ejected as a consequence of material falling on to the supermassive black hole (SMBH) in an AGN. Quite often, the core of the AGN shines brightly at radio wavelengths too. A quintessential example of a radio galaxy in the local Universe – and arguably the first extragalactic radio source discovered – is Cygnus A at a redshift of 0.056 (Baade & Minkowski 1954). In Figure 1.2 a composite image for this radio galaxy with emission at radio (red), X-ray (blue) and optical wavelengths (background) is shown. Cygnus A also shows radio emission from the core of the AGN which is also traced by high-energy X-rays and we elaborate on the various observational signatures from radio galaxies in Section 3.

Many other "local" ($z \sim 0$ radio galaxies displayed morphologies similar to Cygnus A, with their radio lobes extending to hundreds of kiloparsecs. Based on their radio morphology, there were two distinct types of radio galaxies identified. This is the so-called Fanaroff & Riley (1974) classification, where Fanaroff-Riley II (FRII) sources have an edge-brightened morphology and Fanaroff-Riley I (FRI) sources have the peak of emission towards the host galaxy. FRII sources typically have higher radio luminosities. At higher redshifts, radio sources are seen to typically exhibit FRII morphologies and luminosities.

1.2 High-redshift radio galaxies

It was clear that in order to derive meaningful properties of the host galaxies of radio sources, such as the distance, underlying stellar populations, star-formation histories, etc., dedicated imaging and spectroscopic follow-up at optical wavelengths were essential. Spectroscopy of bright radio sources was yielding redshift measurements that were breaking distance records – a redshift of $z = 0.462$ measured by Minkowski (1960) for the radio source 3C 295 was the most distant object known at the time. With the arrival of radio interferometric techniques in the 1950s (such as the Cambridge One-Mile Telescope and Jodrell Bank long-baseline interferometry), precise position measurements for strong radio sources were possible and enabled accurate identification of the host galaxies of radio sources. The first radio galaxy at $z > 1$ was discovered by Spinrad (1982). Chambers et al. (1988) then discovered a radio galaxy at $z > 2$, with the discovery of a $z > 3$ radio galaxy reported only a few months later by Lilly (1988). A couple of years later Chambers et al. (1990) reported the discovery of a radio galaxy at $z = 3.8$. A radio galaxy at $z > 5$ was discovered by van Breugel et al. (1999) at $z = 5.19$, a distance record that was only recently broken by our discovery of a radio galaxy at $z = 5.72$, which is part of this thesis (Saxena et al. 2018a).

Higher sensitivity radio surveys covering larger areas on the sky were discovering orders of magnitude more radio sources, with most of them being low-redshift radio galaxies hosted by ellipticals. The increasing number of radio sources were making dedicated spectroscopic follow-up an expensive exercise. Techniques had to be developed to isolate candidate high-redshift radio galaxies (HzRGs) from these surveys. Miley & De Breuck (2008), in their extensive review of the properties of HzRGs highlight the most commonly used and arguably the most successful selection steps to isolate HzRGs from large radio surveys. In the following we highlight some of the most commonly used and also successful selection techniques for HzRGs.

1.2.1 Selection techniques

Radio colours and spectral indices

The first selection that is often applied to large radio datasets to pick out promising HzRG candidates is to use radio colours or spectral indices to filter out low-redshift radio sources. Radio sources at high-redshifts have been found to exhibit steeper values of the radio spectral index, α, which is defined as $S_\nu \propto \nu^\alpha$, where S_ν is

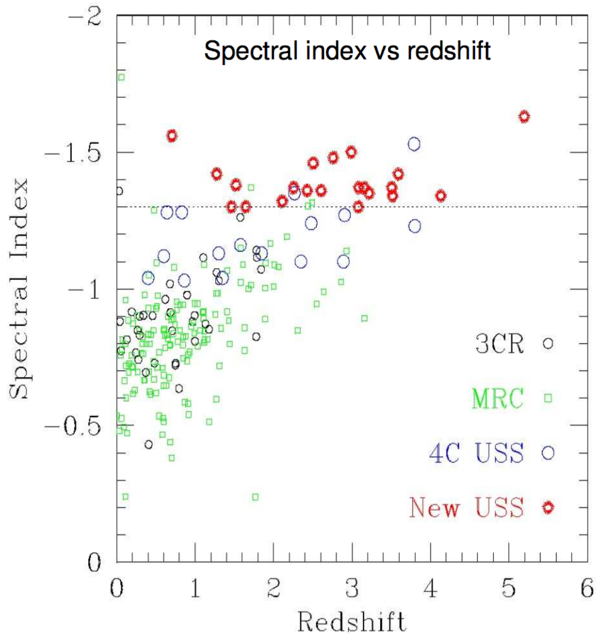

Figure 1.3: The empirically derived correlation between redshift and radio spectral index from De Breuck et al. (2000a). Studies of complete samples have shown that radio sources with steeper spectral indices tend to be at higher redshifts. This has led to the ultra-steep spectrum (USS) selection technique being widely used to shortlist potential HzRGs from large radio datasets.

the flux density at an observing frequency ν. This effect was first investigated by Blumenthal & Miley (1979) and Tielens et al. (1979), where they found that the optical identification fraction in flux limited surveys for steeper spectrum radio sources was lower. Optical faintness serves as a proxy for distance and the lower identification fraction suggested that radio sources with steeper spectral indices are more distant. In Figure 5.10 we show the empirically derived correlation between redshift and spectral index, also known as the $z - \alpha$ correlation, taken from De Breuck et al. (2000a).

Angular size restrictions

The next step is to apply an angular size cut. The motivation to do this largely stems from the observed statistical decrease in angular sizes of radio sources at high redshifts (Miley 1968). This effect was initially observed for radio-loud quasars, but it was soon discovered that extended radio galaxies display such behaviour too (Nilsson et al. 1993). Besides simple geometry, the main reason why sizes of radio sources are expected to decrease at higher redshifts is due to a systematic increase in the density of the ambient medium surrounding these radio galaxies (Barthel & Miley 1988). The higher energy density of the surroundings makes it more difficult for radio jets to grow out to large distances because of increased thrust of radio jets against the ambient medium. Moreover, the substantial increase in the energy density of the cosmic microwave background radiation, that increases as $\propto (1+z)^4$, leads to enhanced inverse Compton losses, extinguishing radio sources earlier in their lifetimes, leading to a statistical decrease in their sizes (Krolik & Chen 1991; Daly 1992).

Optical/infrared faintness

The next step to filter out low-redshift galaxies from a radio survey is to first accurately match the radio data with available optical and infrared data. Once optical/infrared counterparts for radio sources have been identified, the brighter sources may be discarded as they are likely to be lower redshift radio galaxies. The justification of targeting fainter optical/infrared radio sources for spectroscopic follow-up originates from the discovery by Lilly & Longair (1984) that radio galaxies across all redshifts tend to be dominated by an older stellar population, and reside in giant elliptical-like galaxies. This gives rise to a tight correlation between their near-infrared magnitude where light from old stars dominates, and the host galaxy redshift. As a result, near-infrared imaging specifically using the K band was found to be very effective at identifying counterparts of radio sources (see Jarvis et al. 2001b, for example). The same is not true for bluer wavelengths, however, especially at higher redshifts. Lilly & Longair (1984) found substantial deviations at high redshifts for optical to infrared colours, with reported excess of ultraviolet light which they attributed to bursts of star formation.

At very high redshifts ($z \gtrapprox 3$), when the rest frame ultraviolet light redshifts into the optical wavelengths, the 'Lyman break' selection technique may be employed to select high-redshift radio galaxy candidates. This selection essentially relies on the break in the spectrum of a star-forming galaxy produced due to almost complete absorption of radiation by the neutral gas around star-forming regions at wavelengths blueward of the Lyman limit (at 912 Å) (see Steidel et al. 1995, for example). This kind of selection relies on the availability of very deep photometry ($i \gtrapprox 25$ AB) in multiple optical bands, which is hard to achieve over very large areas of the sky (100s of square degrees), the kind of areas that are typically covered by radio surveys. For the largest area radio surveys, it is common practice to identify as promising HzRG candidates only those radio sources that have no optical and/or infrared counterparts in the available all-sky optical and infrared surveys, such as *SDSS* (Alam et al. 2015a), *Pan-STARRS* (Chambers et al. 2016a), *UKIDSS* (Lawrence et al. 2007a) and *WISE* (Wright et al. 2010a).

1.2.2 Follow-up of promising candidates

Once a sample of promising HzRG candidates has been compiled largely following the above mentioned selection criteria, it is then necessary to follow them up at various wavelengths, mainly for spectroscopic redshift measurements but also to study the underlying stellar populations and their environments.

Dedicated deep near-infrared imaging of promising HzRG candidates using the K band filter is an effective way of identifying their host galaxy, as mentioned earlier. Once the host galaxy has been identified or its expected position has been localised, a spectrum may be obtained by placing a long-slit at the appropriate location. Blind spectroscopy at the radio positions has proven to be successful at identifying emission lines originating from the radio galaxy host (see Spinrad 1982, for example). In the future, dedicated integral-field unit (IFU) spectroscopy of promising candidates, which gives a spectrum at every pixel, may help overcome the positional uncertainties that arise due to the lower resolution of radio surveys and could be employed as an effective tool for redshift determination of radio sources.

Once the redshift of a radio source has been determined, it can be followed up at various other wavelengths to shed light on the different physical processes that are underway in distant radio galaxies. In the following Section we first briefly describe the physics of radio and line emission from radio galaxies and then highlight the underlying physical processes that are probed when observing HzRGs at different wavelengths.

1.3 Physics of Radio-loud AGN

In this section, we will briefly describe the key physical processes that are believed to power the large radio lobes originating from AGN and the bright emission lines seen in the ultraviolet, optical and infrared spectra of high-redshift radio galaxies. We will then provide an overview of the pan-chromatic properties of HzRGs and describe the various physical processes that can be probed at different observing wavelengths.

1.3.1 Powering the radio emission

Some of the earliest models to explain the bright radio emission observed from AGN followed the idea that accretion on to the central black hole in an AGN can give rise to twin jets that are perpendicular to the accretion disk and are capable of accelerating particles to relativistic speeds (Blandford & Rees 1974; Scheuer 1974). The presence of strong magnetic fields around the AGN would give rise to radio emission both from the core of the AGN and from the collimated jets (Blandford & Payne 1982). The production of charged particles in the vicinity of the AGN that can then be electromagnetically transported to the poles of the rotating black hole and get accelerated in the jets came to be known as the Blandford-Znajek process (Blandford & Znajek 1977).

Once the jets emanating from the AGN are powered, semi-analytical models describing the growth of FRII type radio sources (as discussed in Section 1.1) can be implemented. These models were primarily constructed to track the growth of radio sources and energy losses due to several physical mechanisms that dominate at different stages of a radio source's lifetime (Kaiser & Alexander 1997; Kaiser et al. 1997; Blundell et al. 1999). The typical lifetime of a radio-loud AGN is $\sim$ 100 Myr (Wan et al. 2000) and the key processes that dominate through the lifetime of a radio AGN are: (i) synchrotron emission in the early stages of radio AGN evolution that also give rise to the power-law behaviour of the low-frequency SED, (ii) adiabatic losses when the jet reaches galactic scales and beyond and finally, (iii) inverse Compton losses due to interaction with the cosmic microwave background (CMB) photons at much larger scales. These processes can be implemented in a cosmological framework using semi-analytical prescriptions and can then be used to estimate the distribution of luminosities, ages and sizes of radio sources at different epochs (see Kaiser & Best 2007, for example).

1.3.2 Powering the rest-frame optical/NIR emission lines

Radio AGN produce a number of rest-frame optical and infrared emission lines. Broadly, a distinction between the emission line spectra exhibited by HzRGs can be made based on the widths of the lines. Classical HzRGs typically exhibit narrow emission lines (FWHM < 2000 km s^{-1}), McCarthy (1993) found that only $\sim 15\%$ of HzRGs show broad emission lines, that are more commonly found in radio-loud quasars where the broad-line region close to the accreting black hole is directly visible. A detailed review of emission lines from HzRGs is presented in McCarthy (1993), and a composite HzRG spectrum presented in this study is shown in Figure 1.4. There are a number of strong emission lines visible in a HzRG spectrum that can be used to infer several important properties about the AGN and the host

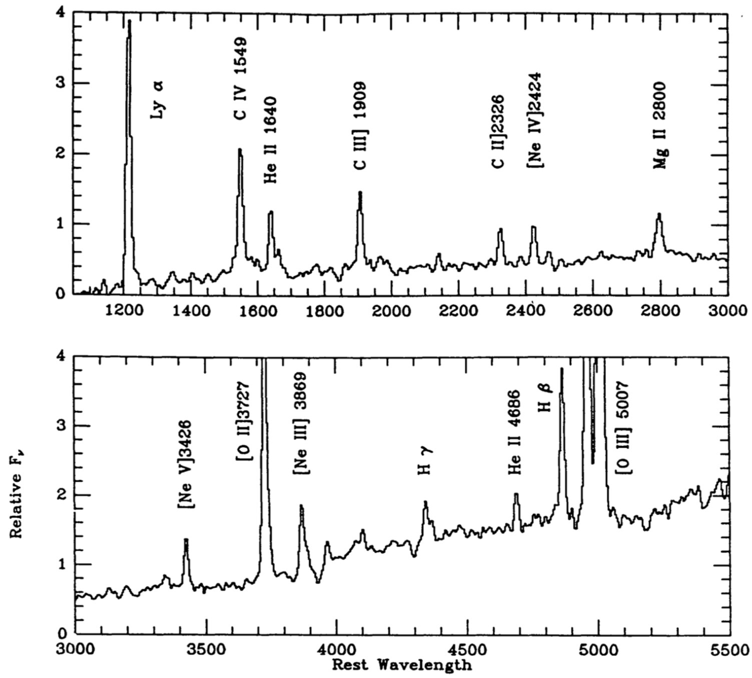

Figure 1.4: Composite HzRG spectrum at rest-frame UV and optical wavelengths, taken from McCarthy (1993). A wide range of broad and narrow emission lines are detected in HzRGs and comparing the line ratios can give insights into the underlying ionising mechanisms.

galaxy, such as ionisation state, metallicity, star-formation rates, etc.

Several ionisation mechanisms have been proposed to explain the observed emission lines. The most direct way to constrain the underlying ionisation mechanism is to compare emission line ratios. McCarthy (1993) found that simple photoionisation models from an AGN spectrum following a power law $\nu^{-1.5}$ were enough to explain the line ratios observed in a large majority of radio galaxies. However, Villar-Martin et al. (1997) showed that the contribution from shocks, which lead to interaction between the radio jet and the line-emitting gas, must also be taken into account when modelling radio galaxy spectra, especially at high redshifts. Best et al. (2000) further showed that for smaller radio sources, shock ionisation due to the radio jet becomes important in explaining the observed spectra. The emerging picture is that in small radio sources the jet is traversing the intergalactic medium of the host galaxy and the shocks associated with the radio jet dominate the ionisation and the kinematics of the emission line gas. In larger radio sources, the shock has passed beyond the line emitting regions and the observed line ratios and kinematics can be explained using simple photoionisation models.

The impact of radio size on the kinematics of the Lyα emission line from HzRGs was shown by van Ojik et al. (1997), where they found that smaller radio sources showed broader Lyα emission lines. This behaviour was again attributed to the interaction between line emitting gas and the radio jet in small radio sources. This result is particularly important for studies of radio galaxies at the highest redshifts, where the rest-frame optical lines are redshifted into the infrared and are harder to observe. However, near-infrared intergral-field spectroscopy of nebular lines for a subsample of the most distant radio galaxies showed complex emission line kinematics, which arise from jet-driven AGN winds and outflows at high redshifts (Nesvadba et al. 2008, 2017).

1.4 A panchromatic view of high-redshift radio galaxies

Having briefly introduced the physics that power the radio emission and the emission lines from gas in radio galaxies, we now discuss the various physical processes that can be studied at different observing wavelengths. Radio galaxies, especially at high redshifts, show remarkable features at almost every wavelength and the relationships and interactions between these constituents make HzRGs excellent probes of galaxy formation and evolution in the early Universe. A lot of the discussion that will follow is derived from the excellent review by Miley & De Breuck (2008). We add in some of the latest observations wherever applicable to sketch a complete picture about HzRGs and their environments. We group the discussion that follows by observing wavelength and then explain the physical processes that contribute to the observed emission at that wavelength. The spectral energy distribution (SED) across a wide range of wavelengths for a radio galaxy at $z = 2.5$, taken from Miley & De Breuck (2008), is shown in Figure 1.5.

1.4.1 Radio

As mentioned already, the bulk of the radio emission observed at low frequencies is powered by non-thermal synchrotron emission emitted by relativistic plasma being accelerated by the central AGN or at the hotspot created by the interaction of the radio jet and the ambient medium, that usually follows a single power law. This single power-law SED is then acted upon by various energy loss processes, such as spectral ageing that affects the radio SED at the high frequencies (Harwood et al. 2013, and references therein) and synchrotron self-absorption at the low frequencies (Callingham et al. 2015, and references therein). As a result, depending on the

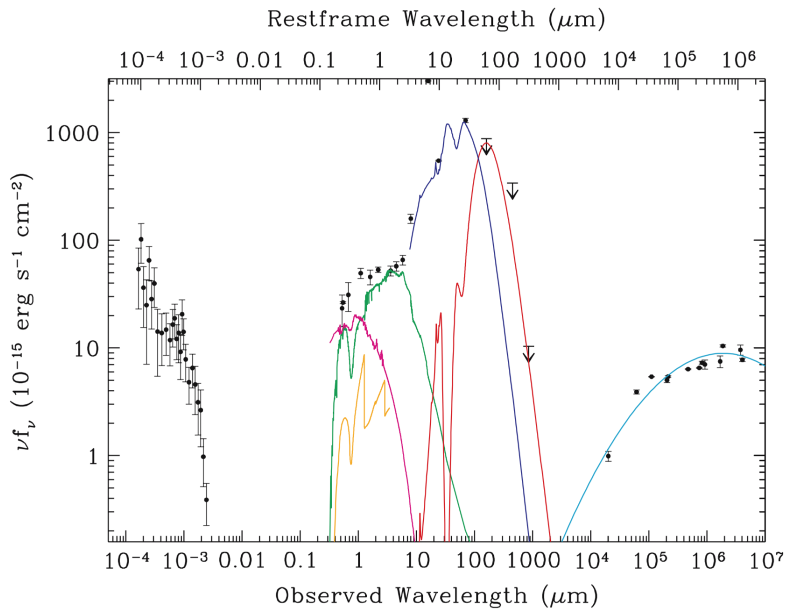

Figure 1.5: A pan-chromatic view of the spectral energy distribution of the HzRG 4C 23.56 at $z = 2.5$, taken from Miley & De Breuck (2008). The solid lines indicate best fitting models to the observations, starting from the highest energies (shortest wavelengths), Black: non-thermal X-ray radiation from the AGN, Green: light from old stars, Yellow: nebular continuum, Magenta: scattered quasar light, Blue: thermal dust emission heated by AGN, Red: thermal dust emission heated by star-bursts, Cyan: radio synchrotron emission.

age and the environment of the radio source, deviations from a single power-law emerge and the SED of radio sources can vary almost on a case by case basis.

1.4.2 Ultraviolet/optical/near-infrared

Studies of radio galaxies at $z > 2$ have shown that the rest-frame ultraviolet (UV) radiation in HzRGs has a strong contribution from light from young stars, but the stellar light is often not enough to account for the total rest-frame UV emission. A significant fraction of the contribution could be attributed to non-stellar emission, such as from an obscured AGN (see Cimatti et al. 1998, for example) or from free-free emission. As discussed already, the UV-optical emission lines shed light on the state of the warm ionised gas and help study properties such as temperature, density, metallicity, ionisation and kinematics of ionised gas. The UV-optical absorption lines probe the cooler atomic gas. The cool atomic gas can also be probed using HI absorption at radio wavelengths (Morganti et al. 2006). At high redshifts

($z > 1.5$), the strong Lyα emission line typically observed in radio galaxy spectra is redshifted into the visible wavelengths, offering an easy way to spectroscopically confirm redshifts of radio sources.

The optical-near infrared (NIR) continuum probes the old stars and is sensitive to the age and formation epoch of the host galaxy (Lilly & Longair 1984). Radio galaxies across all epochs tend to be dominated by an old stellar population (Rocca-Volmerange et al. 2004), which explains the observed correlations between K band magnitudes and redshifts for HzRGs (Jarvis et al. 2001b; Willott et al. 2003). The nebular emission-lines at optical wavelengths have also been used to quantify the excitation state of gas in the radio galaxy, leading to distinct populations of high-excitation and low-excitation radio galaxies (HERGs and LERGs; Best & Heckman 2012). Additionally, emission line ratios are often used to study the nature of the ionising source, as discussed in the previous section.

1.4.3 Mid-infrared/far-infrared/sub-mm

Continuum emission at the mid- to far-infrared wavelengths all the way to sub-mm wavelengths is dominated by thermal dust emission, heated by both the AGN and star-formation activity (van der Werf 1999; Reuland et al. 2004; Seymour et al. 2008). The mid-IR colours of HzRGs have shown that they lie in a similar region as unobscured AGN, and their mid-IR luminosities classify most of them in the category of luminous infrared galaxies (LIRGs) (see Seymour et al. 2007, for example). Observations of HzRGs at 450/850 μm have revealed dust masses of the order of $\sim 10^8\ M_\odot$ and temperatures of $\sim$ 50 K (see Reuland et al. 2004, for example). Although the dust could be heated either by X-rays from the AGN or UV photons from young stars, it is not easy to distinguish one source from the other.

The sub-mm emission lines probe the vast reservoirs of molecular gas, in addition to the dust that is typically present in HzRGs (Emonts et al. 2014, 2016). This molecular gas forms the fuel for intense star-formation activity that is observed in many HzRGs. However, recently **?** showed that the star-formation rates inferred from sub-mm observations of HzRGs may be overestimated, as there may be significant contribution from synchrotron emission extending to these wavelengths. This would mean that hosts of radio AGN lie below the main sequence of star-forming galaxies and many HzRGs may be quenched.

1.4.4 X-rays

Thermal X-ray continuum observations of HzRGs seem to predominantly trace the hot ionised gas that is heated by shocks propagated through the relativistic jets emanating from the AGN, which can often extend to large scales (few 100 kpc) around the central AGN (Carilli 2003; Belsole et al. 2007). Additionally, non-thermal emission from inverse Compton (IC) scattering produced by the same relativistic electron population that contributes to the synchrotron emission is also seen in the X-rays (Schwartz 2002). These components can be seen in blue in Figure 1.2 for a low-redshift radio galaxy. In principle, the energy density of the cosmic microwave background responsible for IC emission increases as $(1 + z)^4$ compensates for the $(1 + z)^{-4}$ decrease in surface brightness, which should make it possible to detect non-thermal X-rays out to higher redshifts (Schwartz 2002).

1.5 Cosmological properties of high-redshift radio galaxies

Having established that HzRGs are exotic objects with a number of physical phenomena visible at various wavelengths, we now turn our attention towards the cosmological implications of HzRGs. HzRGs were initially used as beacons for finding the most distant objects in the Universe and were later found to be surrounded by dense environments. Below we briefly summarise the currently known cosmological properties of HzRGs and their environments.

1.5.1 Number density at high redshifts

Radio galaxies are some of the rarest objects in the Universe. Dunlop & Peacock (1990) reported a rise in the space density of HzRGs compared to the local Universe, with a peak observed around $z \sim 2$. They tentatively observed a decline in their space densities between redshifts of 2 and 4, which other studies have subsequently confirmed (Jarvis et al. 2001a; Rigby et al. 2011, 2015). This behaviour makes radio galaxies at the highest redshifts even rarer, leading to great challenges in identifying and confirming them. Overall, the space density evolution as a function of redshift is very similar to the redshift evolution of the space densities of quasars (see Fan et al. 2004, for example). To further highlight the rarity of HzRGs, only ~ 200 radio galaxies are currently known at $z > 2$ (Miley & De Breuck 2008), which when compared to the number of star-forming galaxies known at $z > 2$ is a minuscule number.

1.5.2 Formation and evolution of massive galaxies across cosmic time

Radio galaxies across a broad range of redshifts form a fairly narrow sequence across the Hubble $K - z$ diagram (Lilly & Longair 1984). Rocca-Volmerange et al. (2004) found that radio galaxies are some of the most massive galaxies at any given epoch in the redshift range $z = 0 - 4$ using detailed stellar population modelling. However, deriving stellar masses from near-infrared photometry has a number of caveats (Miley & De Breuck 2008). First, the K band photometry can often be contaminated by a warm dust component which must be appropriately accounted for. Second, at certain redshifts the K band flux may be contaminated by strong emission lines, which would lead to an overestimation of the stellar mass. Using space based observatories, such as *Spitzer*, that help probe the rest frame infrared wavelengths, Seymour et al. (2007) were able to successfully decompose the optical to infrared SEDs of HzRGs to properly account for the light emitted by old stars. They found that once contaminants are accounted for, a large majority of radio galaxies have stellar masses in the range $10^{10} - 10^{11}\ M_{\odot}$ even at the highest redshifts ($z \sim 4$), putting radio galaxies truly at the most massive end of the galaxy stellar mass function across cosmic time. Therefore, studies of the cosmological evolution of radio galaxies offer a way to understand the physical processes that help shape the most massive galaxies in the Universe.

1.5.3 AGN feedback

The close correlations observed between the supermassive black hole (SMBH) mass and the velocity dispersion of bulges of massive galaxies has shown that the growth of the SMBH directly influences and regulates the growth of the host galaxy (Kormendy & Gebhardt 2001; Merritt & Ferrarese 2001). Therefore, thermal and kinematic feedback from AGN, or simply AGN feedback, must play an important role in galaxy evolution. Without heating of the intergalactic medium through AGN feedback, the Brightest Cluster Galaxies (BCGs), the massive galaxies that reside in the centres of clusters, would encounter runaway star formation through accretion of cold gas and would appear to be even more massive. These BCGs are almost always associated with radio galaxies (see Hogan et al. 2015, for example), showing studies of radio galaxies and their environments are essential to understand the physics of AGN feedback and its impact. For an in-depth review of the observational evidence of AGN feedback, we direct the readers to Fabian (2012).

To match models to the observed distribution of galaxy stellar masses (the galaxy stellar mass function) over redshifts, proper understanding of the feedback physics is essential. At lower stellar masses, feedback from supernovae going off in star-forming regions is enough to heat the gas or move it away through winds, thereby terminating star-formation and regulating the growth of lower mass galaxies. In the most massive galaxies that harbour massive SMBHs, the process of quenching star-formation is undertaken by AGN feedback. Owing to limitations in resolution, state-of-the-art cosmological simulations such as EAGLE (Schaye et al. 2015) rely on calibration of sub-grid physics involving AGN feedback efficiency (Wagner et al. 2012, and references therein) to accurately reproduce the galaxy stellar mass function in the local Universe. To enable modelling of these sub-grid physics from first principles in future simulations, achieving a complete understanding of the role played by AGN feedback in regulating galaxy growth is crucial. A statistically significant sample of radio galaxies and observations of their environments across a broad range of redshifts would help understand this process.

1.5.4 Large scale structure formation

As mentioned in the previous section, radio galaxies are often found at the centres of massive galaxy clusters at low redshifts. From a cosmological point of view, galaxy clusters are crucial to tracing the formation of the most massive dark matter halos, galaxies and supermassive black holes (see Springel et al. 2005, for example). In hierarchical structure formation models, small gravitational instabilities in the early Universe eventually lead to the formation of structure at the largest scales, leading to the emergence of clusters and super-clusters of galaxies in the present day Universe. Therefore, studying the growth and evolution of clusters of galaxies across cosmic time can shed light on the large-scale structure formation history of the Universe. Additionally, the role that a galaxy's environment plays on its evolution requires statistical studies of over-dense regions at high redshifts. Observations of galaxy clusters and proto-clusters also serve as a tool to test fundamental cosmological parameters using simulations, by comparing their number densities, masses and density profiles at different redshifts (Overzier 2016).

Even at high redshifts, radio galaxies are found to lie in the centres of over-dense regions (Pentericci et al. 2000; Venemans et al. 2002, 2007; Overzier et al. 2006; Hatch et al. 2011). Through the Clusters Around Radio-loud AGN (CARLA) survey, Hatch et al. (2014) confirmed that radio galaxies are likely to lie in the centres of clusters and proto-clusters across redshifts. A prime example of a radio galaxy at high redshift, situated in an over-dense environment, orchestrating the formation of proto-clusters is MRC 1138−262, also referred to as the 'Spiderweb Galaxy' (Miley et al. 2006) which is shown in Figure 1.6. The UV/optical image shows numerous satellite galaxies orbiting and merging with the central radio galaxy, which will eventually evolve to become a dominant cluster galaxy, like those observed in clusters in the local Universe. Hunting for bright radio galaxies at higher redshifts is the best way to spot over-dense regions in the early Universe and constrain the growth of these over-densities across cosmic time, testing hierarchical structure formation models.

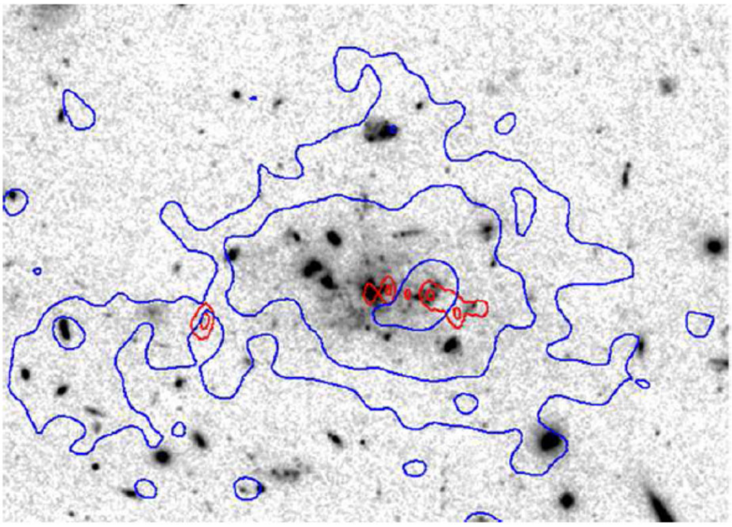

Figure 1.6: Deep HST image of MRC 1138−262, also known as the 'Spiderweb Galaxy' at $z = 2.2$, which is a quintessential example of a proto-cluster surrounding a radio galaxy (Miley et al. 2006). Superimposed on the image are Lyα contours (blue) and radio 8 GHz contours (red). The image shows almost 10 star-forming satellite galaxies in the process of merging with the progenitor of what would go on to become a dominant cluster galaxy in the centre.

1.5.5 Probes of the epoch of reionisation

At $z \geqslant 6$, into the epoch when the Universe was making a phase transition from neutral to completely ionised, bright radio galaxies have the potential to be unique probes of this important cosmological event. At $z \approx 1100$, roughly 400,000 years after the Big Bang, electrons and protons were decoupled from photons, leaving behind a signature in the form of the cosmic microwave background radiation (CMB). As the Universe cooled further, the electrons and protons combined to form neutral hydrogen atoms that pervaded the Universe, giving rise to the so-called 'Dark Ages'. Once the Universe was cool enough for stars and galaxies to start forming, their was light in the Universe and these sources of ultraviolet radiation started ionising the neutral hydrogen around them (Zaroubi 2013). There are many observational signatures showing that the process of reionisation of the Universe was more or less complete by $z \approx 6$. The most important of these are the observations of the Gunn-Peterson trough in the spectra of $z > 6$ quasars (see Becker et al. 2001, for example), which almost completely suppresses flux blueward of the Lyman α line due to absorption by intergalactic neutral hydrogen, an effect that was first predicted by Gunn & Peterson (1965). The fine details about when the pro-

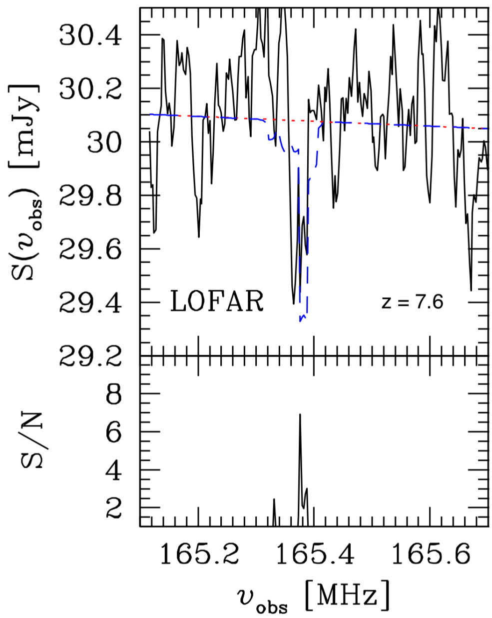

Figure 1.7: Simulated spectrum of a ~ 30 mJy radio source at $z = 7.6$ showing a 21cm absorption feature (Ciardi et al. 2015) from the neutral hydrogen in the intergalactic medium. This simulation shows results with 1000 hours of integration time on LOFAR. The absorption at slightly different wavelengths due to neutral hydrogen clouds in the line-of-sight can give rise to a 21cm forest, which can be studied to constrain the reionisation process over time.

cess of reionisation started and unfolded, and which were the primary sources that drove this process (star-forming galaxies or AGN?) are still unknown and pose an exciting challenge in observational Cosmology today.

One diagnostic that offers the best chance of directly observing the neutral hydrogen at $z > 6$ is the 21cm hyperfine transition line of neutral hydrogen. At $z > 6$, this line is redshifted into the low radio frequency regime ($v_{\rm obs} < 200$ MHz), which can potentially be observed as absorption signals in the spectra of luminous background radio sources that illuminate the line-of-sight (Carilli et al. 2002b). Such a signal is principle observable by the Low Frequency Array (LOFAR; van Haarlem et al. 2013), as shown by Ciardi et al. (2015) and also in Figure 1.7. For a bright radio source at $z > 6$, the radio emission may be absorbed by patches of neutral hydrogen populating the line-of-sight, giving rise to a 21cm forest, similar to the Lyman α forest that is observed in the UV spectra of bright high-redshift quasars.

The biggest challenge at the moment is finding a bright radio source at $z > 6$.

As mentioned earlier, the space density of radio sources decreases dramatically at high redshifts and it is unclear whether bright radio galaxies exist at all at $z > 6$. The detection of distant radio galaxies formed the main motivation behind this thesis, and in the next section we highlight the steps taken through this thesis towards bringing us just a little closer to the epoch of reionisation, as far as radio galaxies are concerned.

1.6 This thesis

The main goal of this thesis is to take advantage of the newer, deeper radio surveys of the sky at low frequencies and detect massive radio galaxies close to or even into the epoch of reionisation, and understand better the physics of galaxy formation and evolution as well as the implications for the reionisation of the Universe. To gain an overall understanding of very distant radio galaxies, this thesis contains a combination of theoretical work, observational work at radio, optical and infrared wavelengths as well as some modelling to interpret those observations. The observations presented in this thesis have been taken from a number of state-of-the-art facilities around the world, namely the *Karl G. Jansky Very Large Array (VLA), William Herschel Telescope (WHT), Large Binocular Telescope (LBT), Gemini North Telescope, Hobby-Eberly Telescope (HET), Gran Telescopio Canarias (GTC)* and the *Very Large Telescope (VLT)*. Below we provide a short description of each chapter of this thesis.

In **Chapter 2** we model the growth of radio sources to predict the expected number of bright radio galaxies at $z \sim 6$, which could be used as effective probes of the epoch of reionisation. We begin by constructing a model that uses masses of supermassive black holes, their accretion rates and spins to calculate jet powers and associated radio luminosities. As these radio sources grow, they lose energy due to various physical processes, the prescriptions for which we put into our model. Running the model for a certain period of time at any epoch, we can predict the space density distribution of radio sources, i.e. the radio luminosity function, along with the distribution of radio source sizes. We first test our model at $z = 2$, where ample radio data is available and show that our predictions match the observations well. We then run our model at $z = 6$ and predict the radio luminosity function and radio size distribution for galaxies at this redshift. We then use this information to define best observing strategies that would help maximise the number of $z = 6$ radio galaxies detected (essentially a coverage area vs. depth trade-off), in a bid to address the first major question faced by studies of distant radio galaxies: ***How many radio galaxies actually exist at*** $z \geqslant 6$ ***and how to find them?***.

In **Chapter 3** we present initial results from an observational campaign to discover fainter radio galaxies across all redshifts. Promising faint high-redshift radio galaxy candidates were selected at 150 MHz using the selection techniques mentioned earlier in this Introduction. For the final sample of 32 promising candidates, we present high-resolution radio observations using the VLA. We also present the overall optical and infrared properties of the sample, and determine photometric redshifts for a handful of sources that have deeper photometry at optical/IR wavelengths. We present radio properties of the sample, including whether the low-frequency radio spectra show signs of curvature, which is often seen in HzRGs. We also report the serendipitous discovery of a giant radio galaxy (GRG) with a photometric redshift of 1.8 ± 0.5. This chapter addresses the question: ***How successful can deeper radio surveys be at identifying distant radio galaxies?***

In **Chapter 4** we present results from a spectroscopic campaign to confirm the redshifts of promising candidates presented in Chapter 3. We are able to identify radio galaxies across a range of redshifts that are almost an order of magnitude fainter in radio luminosity than those previously discovered. We also present near-infrared imaging for of a subset of these confirmed sources to estimate their stellar masses. Next, we select known $z \geqslant 2$ radio galaxies from the literature and add our newly discovered galaxies to form an extended HzRG sample. We then look at the radio and emission line properties of this extended sample, find correlations between many of these properties and introduce scenarios that address open questions surrounding AGN feedback at high redshift. This chapter addresses the question: ***What is the nature of radio galaxies located at the highest redshifts?***

In **Chapter 5** we report the discovery of the most distant radio galaxy known to date, TGSS J1530+1049 at $z = 5.72$, which is very close to the presumed end of the epoch of reionisation. This galaxy was initially selected as a promising radio source in Chapter 2 and subsequent spectroscopic observations and near-infrared photometry helped confirm its high redshift. This discovery breaks the previous record of the most distant radio galaxy, which had been held for almost 20 years. In this Chapter we present a detailed analysis of the Lyα emission line from the host galaxy and how its Lyα and radio properties (such as luminosity and size) compare with other radio sources at high redshifts as well as 'non-radio' galaxies at a similar redshift. We also set estimates on the stellar mass of the host galaxy and show that TGSS J1530+1049 must be a very young radio source. This Chapter takes the first step towards addressing the question: ***How does a radio galaxy very close to the epoch of reionisation look like?***

1.7 Outlook

Radio astronomy is currently undergoing a Renaissance, with state-of-the-art radio telescopes such as the *Low Frequency Array (LOFAR)* and in the near future, the *Square Kilometer Array (SKA)*, that will provide larger sky coverage, higher sensitivities and better angular resolutions over large areas on the sky. These new datasets will open up new parameter spaces that will be used to detect fainter radio galaxies at the highest redshifts. The challenge still remains to detect a radio galaxy at $z > 6$ to enable studying the epoch of reionisation in unparalleled detail, and these new radio surveys are expected to detect a number of such sources. Detection of distant radio galaxies will be especially aided by large area surveys at the lowest frequencies, such as the LOFAR LBA survey at 60 MHz. The advantages of going down to lower radio frequencies are: (i) owing to the steepness of the radio spectral index of HzRGs, they should be much easier to detect at low frequencies, and (ii) a flux density point at lower frequencies will enable additional selection criteria, that do not necessarily rely on the steepness of the spectral indices but can also take advantage of spectral curvature that is characteristic of radio galaxies at the highest redshifts.

From a multi-wavelength point of view, the deeper all-sky optical and infrared surveys using telescopes such as the *Large Synoptic Survey Telescope (LSST)*, *Euclid* and *Wide Field Infrared Survey Telescope (WFIRST)* would enable the identification of the host galaxies of an increasingly large number of radio sources. Additionally, this deeper ancillary data would accelerate searches for the most distant radio AGN as well as their host galaxies and environment. The highly accurate photometric redshifts derived from these surveys would enable studying the redshift evolution of large samples of radio galaxies to higher redshifts, without the explicit need for spectroscopically confirming each of them. For the highest redshift sources, the *James Webb Space Telescope (JWST)* would enable deep near-infrared spectroscopy, shedding light on the ionising mechanisms, the interactions of jets with the ambient interstellar media in host galaxies as well as constraining feedback processes in powerful AGN in the early Universe. Current generation facilities such as the *Atacama Large Millimeter Array (ALMA)* are already enabling studies of molecular gas and outflows at the highest redshifts in a bid to constrain the role played by AGN feedback, and the *Next Generation Very Large Array (ngVLA)* will help probe the cold gas in AGN to even higher redshifts and sensitivities.

The future of detailed studies of radio galaxies at the highest redshifts seems bright.